Peltier effect in normal-metal–superconductor microcontacts

A. Bardas and D. Averin
Department of Physics, State University of New York at Stony Brook, Stony Brook, New York 11794
(Received 22 May 1995; revised manuscript received 23 June 1995)

We have calculated the heat current in the normal-metal–insulator–superconductor contacts with arbitrary transparency of the insulator barrier. In the tunneling limit (small transparencies), the heat flow out of the normal metal reaches its maximum at temperature $T\simeq 0.3\Delta$. At higher values of transparency, the interplay between single-particle tunneling and Andreev reflection determines optimum transparency which maximizes the density of heat flow out of the normal metal. In clean contacts, the optimum transparency is about 0.1 at $T=0.3\Delta$ and decreases with temperature roughly as $(T/\Delta)^{3/2}$. In disordered contacts, disorder enhances Andreev reflection and shifts the optimum point towards smaller transparencies. The optimal ratio of the barrier resistance to the resistance of the normal electrode is $R_N/R_T\simeq 0.01$ at $T=0.3\Delta$ and decreases with temperature similarly to clean contacts. For disordered contacts we also plot current-voltage characteristics for arbitrary values of the ratio R_N/R_T.

I. INTRODUCTION

The flow of electric current in the normal-metal–insulator–superconductor (NIS) contacts is accompanied by the heat transfer from the normal metal into the superconductor. This principle can be applied to the refrigeration of electrons in the normal metal.[1] (Implicitly, the same principle is used in the enhancement of superconductivity in the SIS'IS structures—see Refs. 2 and 3 and references therein.) The mechanism of the heat transfer in the NIS contacts is the same as that of the well-known Peltier effect in metal–semiconductor contacts—see, e.g., Ref. 4. Due to the energy gap in the superconductor, electrons with higher energies (above the gap) are removed from the normal metal more effectively than those with lower energies. This makes the electron energy distribution sharper, thus decreasing the effective temperature of electron gas in the normal metal.

In the limit of very small transparencies D of the insulator barrier, when the mechanism of electron transport across the barrier is single-particle tunneling, the magnitude of heat flow out of the normal metal increases with transparency. However, at larger transparencies, coherent two-electron tunneling ("Andreev reflection") starts to dominate electron transport and suppress the heat flow. This occurs because in the Andreev reflection electrons with all energies, including those inside the energy gap, are removed from the normal metal. Below we study the crossover between the two regimes and find the optimum transparency which maximizes the heat flow through a unit area of the NS interface. The calculations are carried out in the two cases of contacts with clean and disordered electrodes. It is shown that, in accordance with the general understanding that disorder enhances Andreev reflection,[5–7] in disordered contacts the optimum transparency is shifted towards smaller transparencies with increasing disorder.

II. CLEAN CONTACTS

The model of NIS contact we consider is a constriction between normal metal and superconductor with characteristic dimensions d that are much smaller than the coherence length ξ and inelastic scattering length in the electrodes. Because of the condition $d\ll\xi$, we can neglect variation of the superconducting order parameter Δ in the vicinity of the constriction and solve the problem, assuming that Δ is constant in space up to the NS boundary and is equal to its equilibrium value inside the superconductor.

The properties of such a constriction depend strongly on the relation between d and elastic scattering length ℓ near the junction. In the clean limit ($d\ll\ell$), electron motion in the constriction is naturally decomposed into several uncoupled transverse modes (provided that the NS interface is smooth and conserves transverse momentum). In this case one can follow Blonder, Tinkham, and Klapwijk,[8] and solve the Bogolyubov–de Gennes equations independently for each transverse mode. The basic result of such a solution (for details see, e.g., Ref. 9) is contained in the probabilities of normal (B) and Andreev (A) reflection from the NS interface as functions of the quasiparticle energy ϵ:

$$A(\epsilon)=\frac{D^2|a(\epsilon)|^2}{1-2R\ \mathrm{Re}a^2(\epsilon)+R^2|a(\epsilon)|^4}\,, \tag{1}$$

$$B(\epsilon)=\frac{R(1-2\ \mathrm{Re}a^2(\epsilon)+|a(\epsilon)|^4)}{1-2R\ \mathrm{Re}a^2(\epsilon)+R^2|a(\epsilon)|^4}\,.$$

Here D,R are transmission and reflection probabilities of the insulator barrier, $D+R=1$, which are assumed to be independent of energy on the energy scale given by Δ, and $a(\epsilon)$ is the amplitude of Andreev reflection from the ideal NS interface with $D=1$:

$$a(\epsilon)=\frac{1}{\Delta}\begin{cases}\epsilon-\mathrm{sgn}(\epsilon)(\epsilon^2-\Delta^2)^{1/2}\,, & |\epsilon|>\Delta\,,\\ \epsilon-i(\Delta^2-\epsilon^2)^{1/2}\,, & |\epsilon|<\Delta\,.\end{cases} \tag{2}$$

Using the reflection probabilities (1), we can write the balance equation for energy distribution of electrons moving to and from the NS interface.[8] Energy distribution of electrons $f^+(\epsilon)$ that move from the bulk of the normal metal to

the NS interface is the equilibrium Fermi distribution shifted by eV, $f^+(\epsilon)=f(\epsilon-eV)$. Electrons moving from the interface into the normal metal are produced in three processes: quasiparticles incident from the superconductor are transmitted into the normal metal with the probability $(1-A-B)$; electrons are reflected from the interface with probability B; and holes are Andreev reflected as electrons with probability A. (The latter process can be described in more direct terms as tunneling of Cooper pairs out of the superconductor.) Thus, the energy distribution $f^-(\epsilon)$ of electrons moving into the normal metal is

$$f^-(\epsilon)=A(\epsilon)[1-f^+(-\epsilon)]+B(\epsilon)f^+(\epsilon) +[1-A(\epsilon)-B(\epsilon)]f(\epsilon) . \quad (3)$$

From the thermodynamic relation $dU=dQ+\mu\, dN$ applied to electron gas in the normal metal the heat current j flowing from the normal metal into the superconductor in one (spin-degenerate) transverse mode can be calculated as

$$j=\frac{1}{\pi\hbar}\int d\epsilon(\epsilon-eV)[f^+(\epsilon)-f^-(\epsilon)] . \quad (4)$$

It is straightforward to check that when deviations of electron energy distribution from equilibrium in each electrode are small, Eq. (4) is equivalent to another frequently used expression for the heat current, $j=Th$, where T is the temperature of the electrode and h is the entropy flow.

The last step in the calculation is a summation over transverse modes. We do this summation assuming that the electron motion in the junction is quasiclassical, and that the NS interface is smooth and conserves momentum along it. Then the transmission probability D of the interface depends only on the energy $\epsilon_\perp$ of electron motion across the interface, and can be taken to be $D(\epsilon_\perp)=D_0\exp\{(\epsilon_\perp-\mu)/\epsilon_{tr}\}$. In this expression, D_0 is the transparency at Fermi energy, and ϵ_{tr} is an energy scale associated with electron motion under the barrier, which is assumed to be much larger than the superconducting energy gap. Under these assumptions summation over transverse modes (i.e., over angles of incidence on the interface) gives for the total heat current J

$$J=\frac{N}{\pi\hbar}\int_0^{D_0}\frac{dD}{D}\int d\epsilon(\epsilon-eV)[f^+(\epsilon)-f^-(\epsilon,D)] , \quad (5)$$

where $N=Sm\epsilon_{tr}/\pi\hbar^2$ is the effective number of transverse modes, m is the electron mass, and S is the junction area.

Taking the limit $D\to 0$ in Eqs. (1) and (3), one can see that for $D_0\to 0$, Eq. (5) for the heat current reduces to the form given by the tunnel Hamiltonian approach:

$$J=\frac{1}{e^2R_T}\int_{-\infty}^{+\infty}d\epsilon\Theta(\epsilon^2-\Delta^2)\frac{|\epsilon|(\epsilon-eV)}{\sqrt{\epsilon^2-\Delta^2}}[f(\epsilon-eV)-f(\epsilon)] , \quad (6)$$

where R_T is the normal-state tunneling resistance of the barrier, $R_T^{-1}=Ne^2D_0/\pi\hbar$, and $\Theta(x)$ is the theta function.

Figure 1 shows the heat current as a function of the bias voltage V across the contact for different transparencies D_0 calculated numerically from Eqs. (1), (3), and (5). The curves illustrate how increasing transparency of the barrier suppresses heat transfer out of the normal metal. We see that

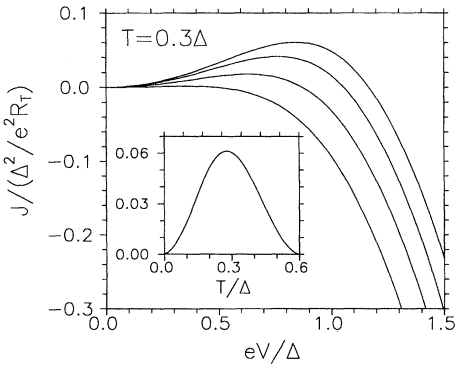

FIG. 1. Heat current J in the clean NIS contact versus bias voltage V for several transparencies D_0 of the insulator barrier calculated from Eq. (5). From top to bottom, $D_0=0$ (tunneling limit), 0.03, 0.1, and 0.2. The inset shows the heat current in the tunneling limit calculated for the optimum bias voltage as a function of temperature; at low temperatures $J\propto(T/\Delta)^{3/2}$.

for each transparency there is an optimal bias voltage which maximizes the heat current J. The inset in Fig. 1 shows J at the optimal bias voltage in the tunneling limit calculated from Eq. (6). The heat current J in this limit is maximum at $T\simeq 0.3\Delta$ and decreases both at small and large temperatures. One can check that at $T\ll\Delta$ the heat current decreases as $(T/\Delta)^{3/2}$.

In Fig. 2 we plot the heat current per one transverse mode at the optimum bias voltage as a function of barrier transparency D_0. At small transparencies the heat current increases linearly with transparency, indicating that we are in the tunneling limit where electron transport is dominated by single-particle tunneling. However, at larger transparencies the heat current starts to decrease with transparency due to the increasing contribution to transport from two-particle tunneling. At the transition point between the two regimes the heat flow out of the normal metal is maximized. A crude estimate of the transparency which corresponds to this transition at low temperatures can be obtained if we compare the amount of heat per transverse mode generated by the two-particle tunneling in the normal electrode, $\simeq(D_0\Delta)^2/\hbar$, with the heat flow out of this electrode in the tunneling regime. As

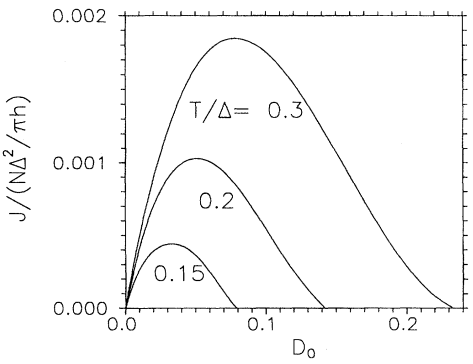

FIG. 2. The maximum heat current density in the clean NIS contact as a function of transparency D_0 of the insulator barrier for several temperatures. For discussion see text.

was noted above, the latter can be estimated as $(T^3\Delta)^{1/2}D_0/\hbar$ (see also inset in Fig. 1). From these estimates we see that at $T \ll \Delta$ the optimal transparency scales as $(T/\Delta)^{3/2}$. This conclusion is in qualitative agreement with Fig. 2.

III. DISORDERED CONTACTS

In this section we consider the same model of a short NIS constriction, but assume that the constriction dimensions d are much larger than the elastic mean free path ℓ in the electrodes. A convenient way to describe such a disordered constriction is provided by the quasiclassical kinetic equations for nonequilibrium Green's function $\check{G}$ of the electrodes.[10–12] Green's function $\check{G}$ is a triangular matrix in the Keldysh space,

$$\check{G}=\begin{pmatrix} \hat{G}^R & \hat{G}^K \\ 0 & \hat{G}^A \end{pmatrix}, \tag{7}$$

where the advanced $\hat{G}^A$, retarded $\hat{G}^R$, and Keldysh component $\hat{G}^K$ are 2×2 matrices in the electron-hole (Nambu) space. The retarded and advanced functions carry information about the excitation spectrum of the system, while the Keldysh function describes the distribution of quasiparticles.

For small constrictions, $d \ll \xi$, we can neglect all but the gradient term in the equation for the Green's function in the vicinity of the constriction, so that the equation is reduced to the diffusion equation[10–12]

$$\vec{\nabla}(\mathscr{D}\check{G}\vec{\nabla}\check{G})=0 , \tag{8}$$

with the diffusion coefficient $\mathscr{D}=\frac{1}{3}v_F\ell$, where v_F is the Fermi velocity. The diffusion equation in the electrodes should be complemented by the boundary condition at the NS interface:[13,14]

$$c\vec{n}\check{G}\vec{\nabla}\check{G}=[\check{G},\check{G}_S] . \tag{9}$$

In this expression, $\vec{n}$ is the vector normal to the NS interface, and $\check{G}$, $\check{G}_S$ are the Green's functions on the normal and superconducting sides of the interface, respectively. The coefficient c describes the interface transparency and can be written as $2\sigma/g$, where $\sigma=2e^2\nu\mathscr{D}$ is the conductivity of the normal metal, and $g=e^2\nu\langle\vec{n}\vec{v}_F D/R\rangle$ is the normal-state conductance per unit area of the interface. Here D and R are the transmission and reflection probabilities of the interface, ν is the density of states at the Fermi level, and $\langle\cdots\rangle$ denotes averaging over angles of incidence on the interface.

On a quantitative level, properties of the constriction depend on its specific geometry. In a simple one-dimensional (1D) model (Fig. 3) considered below, the constriction is represented as a 1D normal conductor of length d, cross-section area A, and resistance $R_N=d/(A\sigma)$, and it is assumed that the contribution of the bulk regions to the total resistance of the structure is much smaller than R_N. In this case we can neglect variations of the order parameter Δ and Green's function $\check{G}_S$ in the superconducting electrode, and assume that Δ and $\check{G}_S$ are equal to their equilibrium values up to the NS boundary:

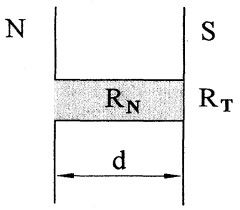

FIG. 3. Schematic diagram of disordered NIS contact. Darker region shows the quasi-1D constriction of length d which determines the resistance R_N of the normal electrode. An insulator barrier with normal-state resistance R_T is placed at the NS interface in the constriction.

$$G_S^{R(A)}=\begin{pmatrix} g^{R(A)} & f^{R(A)} \\ -f^{R(A)} & -g^{R(A)} \end{pmatrix} = \frac{1}{\sqrt{(\epsilon\pm i0)^2-\Delta^2}}\begin{pmatrix} \epsilon & \Delta \\ -\Delta & -\epsilon \end{pmatrix}, \tag{10}$$

$$G_S^K=G_S^R(\epsilon)n(\epsilon)-n(\epsilon)G_S^A(\epsilon), \quad n(\epsilon)=\tanh\left(\frac{\epsilon}{2T}\right) . \tag{11}$$

In the 1D constriction (Fig. 3) the Green's functions depend only on the coordinate x along the constriction, so that the diffusion equation becomes

$$\frac{\partial}{\partial x}\left(\check{G}\frac{\partial}{\partial x}\check{G}\right)=0 . \tag{12}$$

The normalization condition on $\check{G}$, $\check{G}^2=\check{1}$,[12,15] implies that the retarded and advanced components can be parametrized as follows:[16]

$$\hat{G}^{R(A)}(\epsilon)=\pm\{\hat{\sigma}_z\cosh[U^{R(A)}(\epsilon)]+i\hat{\sigma}_y\sinh[U^{R(A)}(\epsilon)]\} , \tag{13}$$

where σ's are Pauli matrices, and upper and lower signs are for $\hat{G}^R$ and $\hat{G}^A$, respectively. The fact that the retarded and advanced functions are nondiagonal indicates the proximity effect in the normal region.

The Green's functions should satisfy the equilibrium boundary condition at the normal end of the constriction ($x=-d$): $\hat{G}^{R(A)}=\pm\hat{\sigma}_z$, i.e., $U^{R(A)}=0$. Equation (12) with this boundary condition determines $U^{R(A)}$: $U^{R(A)}(x)=a^{R(A)}(1+x/d)$, where $a^{R(A)}(\epsilon)\equiv U^{R(A)}(x=0,\epsilon)$. Substituting Eqs. (13) into the boundary condition (9) we reduce it then to a transcendental equation:

$$\pm\frac{R_T}{R_N}a^{R(A)}=f^{R(A)}\cosh a^{R(A)}-g^{R(A)}\sinh a^{R(A)} . \tag{14}$$

Here $g^{R(A)}$ and $f^{R(A)}$ are components of the equilibrium Green's functions (10) of the superconductor, and R_T is the normal-state tunneling resistance of the NS interface, $R_T^{-1}=gA$.

The next step is to find the Keldysh function $\hat{G}^K$ which can be represented as[12]

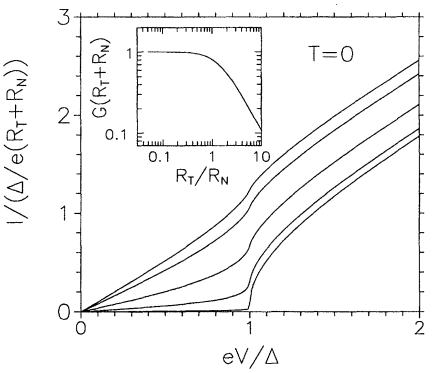

FIG. 4. I-V characteristics of disordered NIS contact at zero temperature and several values of the resistance ratio R_T/R_N. From top to bottom, $R_T/R_N=0$, 1, 3, 10, and 100. The inset shows the linear conductance $G=dI/dV|_{V=0}$ as a function of R_T/R_N. The curves illustrate the transition between the tunneling regime ($R_T>R_N$) characterized by the gap at $V<\Delta/e$ and "metallic" regime ($R_T<R_N$) characterized by large subgap conductance and excess current at $V\gg\Delta/e$.

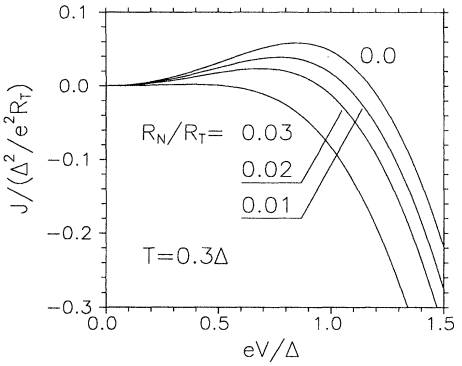

FIG. 5. Heat current J in the disordered NIS contact versus bias voltage V for several ratios of the normal electrode resistance R_N to the resistance R_T of the insulator barrier. As in the clean contacts, the heat current is maximized at $V\simeq\Delta/e$.

$$\hat{G}^K=\hat{G}^R(\epsilon)\hat{h}(\epsilon)-\hat{h}(\epsilon)\hat{G}^A(\epsilon)\ , \tag{15}$$

$$\hat{h}(\epsilon)=f_1(\epsilon)\hat{1}+f_z(\epsilon)\hat{\sigma}_z\ .$$

Equation (12) with the retarded and advanced components (13) gives the following equations for the distribution functions $f_{1(z)}$: $[1+\cosh(U^R\mp U^A)]\partial f_{1(z)}/\partial x=\text{const}\equiv B_{1(z)}/d$. Combining these equations with the boundary condition (9) at $x=0$ and equilibrium boundary condition at $x=-d$, $f_{1,(z)}(-d,\epsilon)=[n(\epsilon-eV)\pm n(\epsilon+eV)]/2$, we find the functions $B_{1,z}$ which determine currents across the NS interface:

$$B_1(\epsilon)=\frac{A_1(\epsilon)}{D_1}[2n(\epsilon)-n(\epsilon-eV)-n(\epsilon+eV)]\ , \tag{16}$$

$$B_z(\epsilon)=\frac{A_z(\epsilon)}{D_z}[n(\epsilon-eV)-n(\epsilon+eV)]\ ,$$

where

$$A_{1(z)}=(g^R-g^A)(\cosh a^R+\cosh a^A)$$
$$-(f^R\mp f^A)(\sinh a^R\pm\sinh a^A)\ ,$$

$$D_{1(z)}=4\left[\frac{R_T}{R_N}+A_{1(z)}(\epsilon)\frac{\tanh[(a^R\mp a^A)/2]}{2(a^R\mp a^A)}\right]\ .$$

Equations (14) and (16) enable us to find electric current and heat current in the NS junction. The electric current can be written as follows:

$$I=\frac{e\nu\mathcal{D}A}{2}\int_{-\infty}^{+\infty}d\epsilon\ \ \mathrm{tr}\{\hat{\sigma}_z[\check{G}\vec{\nabla}\check{G}]^K(\epsilon)\}$$

$$=\frac{1}{2eR_N}\int_{-\infty}^{+\infty}d\epsilon B_z(\epsilon)\ . \tag{17}$$

Figure 4 shows the current I (17) as a function of the bias voltage V at several ratios of the resistances R_T/R_N and vanishing temperature. At large tunnel resistances R_T the I-V characteristic exhibits the gap at $V<\Delta/e$ and singularity at $V=\Delta/e$. At smaller R_T the gap is closed by the increasing contribution to the current from Andreev reflection, but the I-V characteristic still has the singularity (logarithmic divergence of the differential conductance) at $V=\Delta/e$. Transition between the two regimes is clearly visible in the zero-bias linear conductance shown in the inset in Fig. 4. At $R_T<R_N$ the conductance with a good accuracy equals simply $(R_T+R_N)^{-1}$, while at $R_T>R_N$ it decreases as R_N/R_T^2.

Recalling the definition of the heat current used in the previous section and Eq. (17) for the electric current, we can write the following expression for the heat flow out of the normal electrode in the disordered NIS junction:

$$J=\frac{1}{2e^2R_N}\int_{-\infty}^{+\infty}d\epsilon(\epsilon-eV)[B_1(\epsilon)+B_z(\epsilon)]\ . \tag{18}$$

As can be seen from Eqs. (14) and (16), the currents $B_{1,z}$ have the property $B_{1(z)}(-\epsilon)=\mp B_{1(z)}(\epsilon)$. With these relations, Eq. (18) can be rewritten as follows:

$$J=-IV+\frac{1}{e^2R_N}\int_0^{\infty}d\epsilon\epsilon B_1(\epsilon)\ . \tag{19}$$

At $R_T\gg R_N$, both Eq. (17) for the electric current and Eqs. (18) and (19) for the heat current are reduced to the form given by the tunnel Hamiltonian approach. In particular, the heat current J is again given by Eq. (6).

Some results of the numerical calculation of the heat current from Eqs. (14), (16), and (19) are shown in Figs. 5 and 6. We see that the properties of the heat current in disordered contacts are qualitatively similar to those for clean contacts. The heat current density grows with increasing transparency of the tunneling barrier in the regime of small transparencies (large tunnel resistances R_T) and is gradually suppressed at large transparencies. The main difference with the clean case is that the scale of transparencies (in particular, the optimum transparency) is shifted downwards by a small factor ℓ/d, which decreases with increasing resistance of the normal electrode. The physical reason for this shift is that disorder in

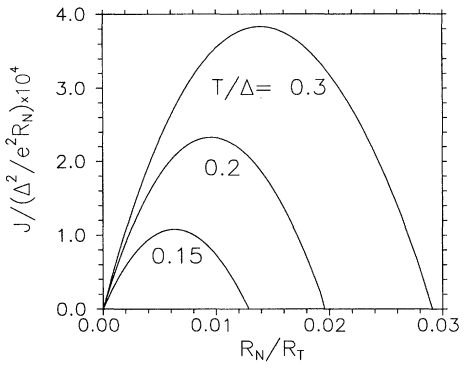

FIG. 6. The heat current density in the disordered NIS contact calculated at the optimum bias voltage as a function of the insulator barrier resistance R_T. The curves are similar to those in Fig. 2 for clean contacts. Note, however, that the scale of the x axis, R_N/R_T, for disordered contacts corresponds to much smaller transparencies of the tunnel barrier than for clean contacts $[R_N/R_T \simeq (d/\ell) D_0 \gg D_0]$.

the normal electrode enhances the contribution of Andreev reflection to transport and therefore suppresses the heat flow out of the normal metal.

IV. CONCLUSION

In conclusion, we have calculated the heat current in clean and disordered NIS microcontacts which is caused by electric current flow across the NS interface. The mechanism of the heat transfer is analogous to that of the Peltier effect in normal-metal–semiconductor structures. Results for clean NIS junctions are obtained by solving the Bogolyubov–de Gennes equations. Disordered junctions are described with the quasiclassical equations for nonequilibrium Green's functions of the electrodes. In both cases the heat current density exhibits nonmonotonic dependence on the interface transparency, increasing at small transparencies and decreasing at large transparencies. The transition between the two regimes takes place at the transparency which is determined by the interplay of single-particle tunneling and Andreev reflection.

At intermediate temperatures, $T \simeq \Delta$, this transition occurs at the transparencies which are larger than the barrier transparencies of the typical tunnel junctions between good metals. For instance, even quite small specific tunneling resistance on the order of 10 $\Omega \times \mu m^2$ corresponds to barrier transparency $\simeq 10^{-4}$. However, as was demonstrated above, as temperature decreases, the transition point moves rapidly towards smaller transparencies, and at low temperatures finite barrier transparency can pose an important limitation on the refrigeration power of NIS junctions. As follows from our estimates in Sec. II, in the clean case transparency-related limitation should become important at $T \simeq 0.01\Delta$ in junctions with specific resistance 10 $\Omega \times \mu m^2$ or less.

The authors gratefully acknowledge discussions with K. Likharev. This work was supported in part by ONR Grant No. N00014-95-1-0762.

[1] M. Nahum, T.M. Eiles, and J.M. Martinis, Appl. Phys. Lett. **65**, 3123 (1994).
[2] M.G. Blamire, E.C.G. Kirk, J.E. Evetts, and T.M. Klapwijk, Phys. Rev. Lett. **66**, 220 (1991); D.R. Helsinga and T.M. Klapwijk, Phys. Rev. B **47**, 5157 (1993).
[3] A.V. Zaitsev, JETP Lett. **55**, 66 (1992).
[4] K. Seeger, *Semiconductor Physics* (Springer, New York, 1991), Chap. 4.
[5] A.F. Volkov, A.V. Zaitzev, and T.M Klapwijk, Physica C **210**, 21 (1993).
[6] C.W.J. Beenakker, B. Rejaei, and J.A. Melsen, Phys. Rev. Lett. **72**, 2470 (1994).
[7] Yu.V. Nazarov, Phys. Rev. Lett. **73**, 1420 (1994).
[8] G.E. Blonder, M. Tinkham, and T.M. Klapwijk, Phys. Rev. B **25**, 4515 (1982).
[9] C.W.J. Beenakker, in *Mesoscopic Quantum Physics*, edited by E. Akkermans, G. Montambaux, and J.-L. Pichard (North-Holland, Amsterdam, in press).
[10] G. Eilenberger, Z. Phys. **214**, 185 (1968).
[11] K. Usadell, Phys. Rev. Lett. **25**, 507 (1970).
[12] A.I. Larkin and Yu.N. Ovchinnikov, Sov. Phys. JETP **41**, 960 (1975); **46**, 155 (1977).
[13] A.V. Zaitsev, Sov. Phys. JETP **59**, 1015 (1984).
[14] M.Yu. Kuprianov and V.F. Lukichev, Sov. Phys. JETP **67**, 1163 (1988).
[15] A.L. Shelankov, J. Low Temp. Phys. **60**, 29 (1985).
[16] A.F. Volkov, JETP Lett. **55**, 474 (1992).

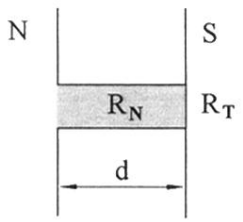

FIG. 3. Schematic diagram of disordered NIS contact. Darker region shows the quasi-1D constriction of length d which determines the resistance R_N of the normal electrode. An insulator barrier with normal-state resistance R_T is placed at the NS interface in the constriction.